OPEN

Light: Science & Applications (2014) 3, e181; doi:10.1038/lsa.2014.62

www.nature.com/lsa

ORIGINAL ARTICLE

An electrophosphorescent organic light emitting concentrator

Jaesang Lee[1], Michael Slootsky[2], Kyusang Lee[1], Yifan Zhang[2] and Stephen R Forrest[1,2,3]

We demonstrate threefold directional light concentration from an organic light-emitting diode luminaire for use in spot lighting and other applications where high intensity illumination is required. The concentrating luminaire comprises four triangular, large-area green electrophosphorescent organic light emitting diodes (PHOLEDs) deposited on plastic substrates and assembled into a pyramidal structure with an open base that serves as the light exit aperture. The PHOLED surfaces are highly reflective to direct the emission from the devices to the aperture independent of the original emission position within the pyramid. The far-field intensity profile of the concentrator has a 'batwing' distribution that meets the requirements for general lighting for uniform illumination of planar surfaces.
Light: Science & Applications (2014) **3,** e181; doi:10.1038/lsa.2014.62; published online 20 June 2014

Keywords: large-area PHOLED; luminaire; phosphorescence; plastic substrates

INTRODUCTION

The potential of phosphorescent organic light emitting diodes (PHOLEDs) has been substantiated by their successful commercialization in flat panel displays.[1,2] More recently, PHOLEDs have found applications in solid-state lighting due to their color tunability and low cost.[3] For use in general lighting, however, PHOLEDs must operate at a higher luminance (>3000 nits) than they would in flat panel displays. To obtain this level of brightness, current densities >1 mA cm^{-2} are required, which can reduce the PHOLED lifetime and efficiency.[4,5] Moreover, to obtain a desirable light distribution profile for uniform surface illumination, additional optical lighting source solutions[6–8] are required that often increase the cost and complexity of the fixture.

Here, we demonstrate concentrated electroluminescence in a pattern that provides uniform surface illumination using an integrated PHOLED light concentrating luminaire. The luminaire comprises four triangular, green emitting PHOLEDs assembled into a pyramidal structure with an open base that forms the exit aperture. The reflectance inherent to the PHOLED architecture concentrates light emitted into the structure by the opposing pyramidal sides, ultimately directing the emission toward the aperture. Because the emissive area is larger than that of the aperture, the luminance is increased by approximately a factor of three compared to a conventional device with the same aperture area. The far-field intensity profile of the concentrator exhibits a 'batwing' distribution that is desirable in many illumination applications. The directionality of the emission from the PHOLEDs determines the radiation pattern of the concentrator and also affects the degree of light concentration.

MATERIALS AND METHODS

An illustration of the concentrator with a schematic of the PHOLEDs is shown in Figure 1. Four PHOLEDs grown on triangular, indium tin oxide (ITO)-coated polyethylene terephthalate substrates (Sigma-Aldrich, St. Louis, MO, USA) were attached to metal plates of the same shape and size as the PHOLEDs. Each section, comprising both the device and the plate (Figure 1c), was then assembled into a pyramidal structure with an apex angle of 15.5°. The sections were fixed in place using tape. The emissive (or substrate) side of each PHOLED faced inwards so that the light emitted from one segment was reflected by the adjacent devices. The light was eventually directed towards the exit aperture (see Figure 1d and Supplementary Movie S1).

The PHOLEDs were grown by vacuum sublimation at a base pressure of $<5\times10^{-7}$ Torr on 60 Ω $square^{-1}$ ITO-coated substrates with >79% transmittance at λ=550 nm. The device structure was as follows: ITO (100 nm)/MoO_3 doped at 15 vol.-% in 4,4'-bis(carbazol-9-yl)biphenyl (CBP) as a hole injection layer[9,10] (60 nm)/CBP as the hole transport layer (10 nm)/bis(2-phenylpyridine)(acetylacetonate)iridium(III) ($Ir(ppy)_2(acac)$) doped at 8 vol.-% in CBP as the emissive layer (15 nm)/2,2',2''-(1,3,5-benzinetriyl)-tris(1-phenyl-1-H-benzimidazole) (TPBi) as the hole blocking and electron transporting layer[11] (65 nm)/LiF (1.5 nm)/Al (cathode, 100 nm). The areas of the reference PHOLED and one triangular side of the concentrator were 1 cm^2 and 1.85 cm^2, respectively, resulting in a total concentrator interior area of 7.4 cm^2. Prior to deposition, the particulates remaining on the solvent-cleaned substrates were removed by CO_2 snow cleaning to minimize electrical shorts.[12] PHOLED electroluminescence characteristics were measured using a parameter analyzer and a calibrated Si-photodiode with an area larger than that of the concentrator aperture.[13]

[1]Department of Electrical Engineering and Computer Science, University of Michigan, Ann Arbor, MI, USA; [2]Department of Physics, University of Michigan, Ann Arbor, MI, USA and [3]Department of Materials Science and Engineering, University of Michigan, Ann Arbor, MI, USA
Correspondence: Dr SR Forrest, Department of Electrical Engineering and Computer Science, University of Michigan, Ann Arbor, MI, USA
E-mail: stevefor@umich.edu
Received 26 February 2014; revised 27 March 2014; accepted 31 March 2014

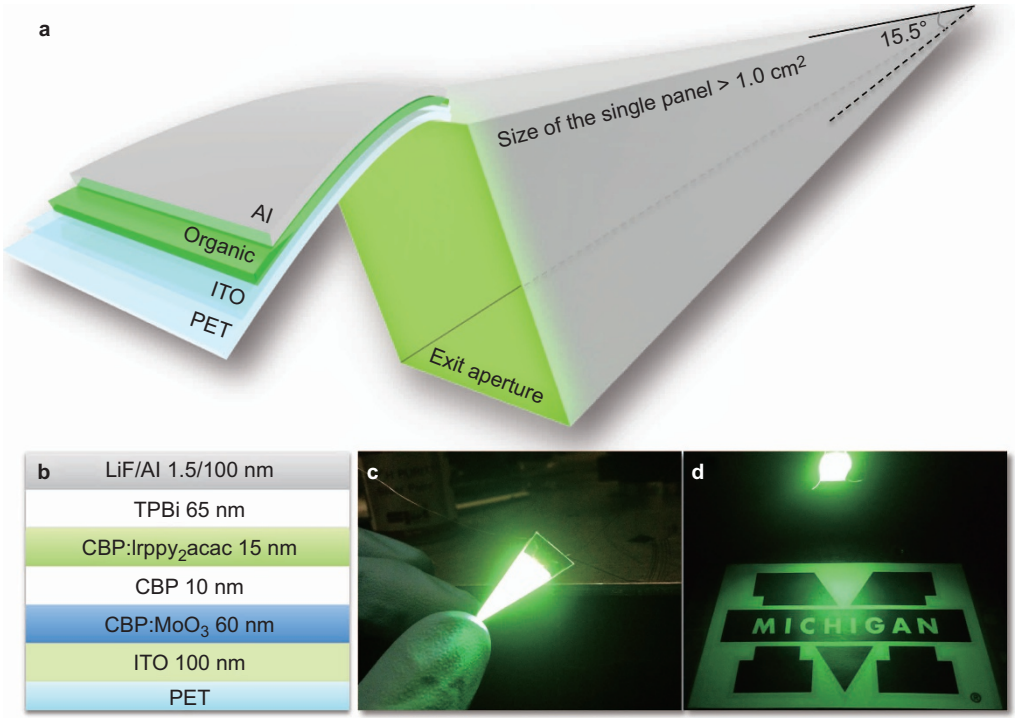

Figure 1 (**a**) Illustration of the concentrator. (**b**) The green PHOLED structure. (**c**) Photograph showing the emission from a single panel PHOLED and (**d**) from a four-sided concentrator. PHOLED, phosphorescent organic light emitting device.

RESULTS AND DISCUSSION

The concentration factor (*CF*), i.e., the ratio of the luminous flux of the luminaire measured at the exit aperture to that of the conventional planar reference device with the same area *as the aperture*, is expressed as:

$$CF(J) = \frac{\sum_{i=1}^{4} L_{\mathrm{side},i}(J) \times A_{\mathrm{side}}}{L_{\mathrm{ref}}(J) \times A_{\mathrm{ref}}} \qquad (1)$$

Here, $L_{\mathrm{side},i}$ and L_{ref} are the luminance values from the single panel concentrator device placed within the luminaire and the reference device (areas: A_{side} and A_{ref}), respectively, at current density J. We define

$$L_{\mathrm{eff}} = \sum_{i=1}^{4} L_{\mathrm{side},i}\left(A_{\mathrm{side}}/A_{\mathrm{ref}}\right)$$

as the effective luminance of the concentrator emitted at the aperture compared with the reference.

Figure 2a shows the L_{eff}–J characteristics of the reference device, a concentrator with only one panel turned on, and from the concentrator with all four sides active. The J–V characteristics (inset) indicate that the panel device operates at a higher voltage than the reference,

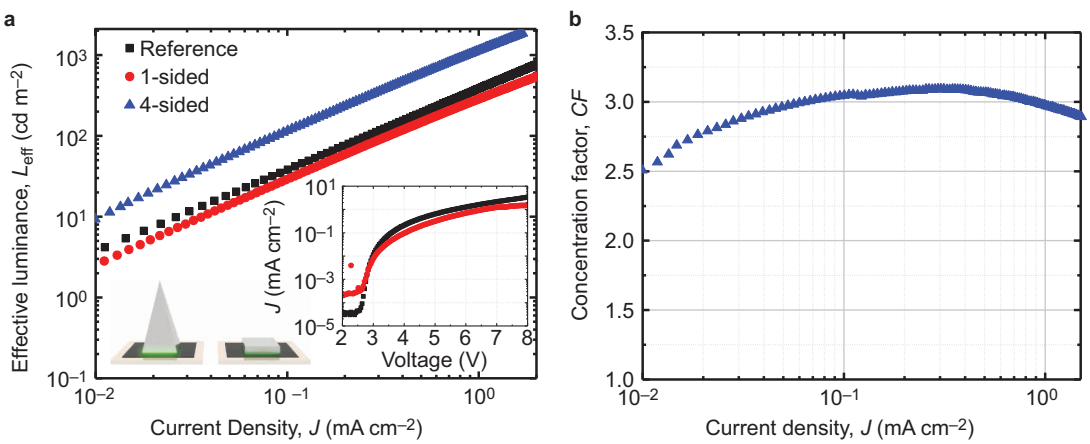

Figure 2 (**a**) Effective luminance *vs.* current density (L_{eff}–J) characteristics of the reference device (squares), a single panel device (circles), and the four-sided device forming the concentrator (triangles). Inset: current density *vs.* voltage (J–V) characteristics of the reference device and a single-panel PHOLED. (**b**) *CF vs. J* of the concentrator. *CF*, concentration factor; PHOLED, phosphorescent organic light emitting device.

doi:10.1038/lsa.2014.62

which primarily results from the increased lateral resistance of ITO with increased device area.[14,15] Although the single panel device has a lower L_{eff} than the reference due to losses from reflections inside the concentrator, the integrated L_{eff} from the concentrator substantially exceeds that of the reference. As a result, the *CF* is 2.5 to 3.1 at current densities from 0.01 to 1 mA cm^{-2}, as shown in Figure 2b. Given the area ratio of 7.4, the loss in the concentrator is approximately 60%. However, this loss is partially compensated by the higher brightness at the aperture.

To investigate the effect of geometry on the *CF*, we can rewrite Equation (1) as

$$CF(J)=4G(\theta_{apex})\times\eta_{ext}[J,G(\theta_{apex})] \quad (2)$$

where $G(\theta_{apex})=\frac{1}{4}\csc(\theta_{apex}/2)$ is the geometric area ratio between the single concentrator panel and the aperture as a function of apex angle θ_{apex}. Additionally, $\eta_{ext}[J,G(\theta_{apex})]$ is the geometric extraction efficiency measured by comparing the luminance of a single panel concentrator device with the reference at *J*. Thus,

$$\eta_{ext}\left[J,G(\theta_{apex})\right]=\int_S I(s)R(\theta_{apex})^{N_{ds}}\mathrm{d}s \Big/ \int_S I(s)\mathrm{d}s \quad (3)$$

where $I(s)$ is the initial luminance emitted by an area segment, d*s*, of the single panel device with a total area of *S*, $R(\theta_{apex})$ is the reflectance of the PHOLED and N_{ds} is the number of reflections for a ray from d*s* to reach the aperture, as discussed below. Figure 3 provides *G*, η_{ext} and *CF* at $J=1.0$ mA cm^{-2} as functions of four different θ_{apex} and a fixed aperture area of 1.0 cm^2. As θ_{apex} decreases from 55.5° to 15.5°, η_{ext} decreases from 68.1%±1.5% to 38.9%±1.3% due to the increased number of reflections. This suggests that the effective area that contributes to the output luminance decreases with θ_{apex}. Nonetheless, the *CF* increases from 1.46±0.03 to 2.92±0.10 due to the dramatic increase in *G*. Table 1 gives the values for *CF* and η_{ext} at $J=1.0$ mA cm^{-2} for these devices.

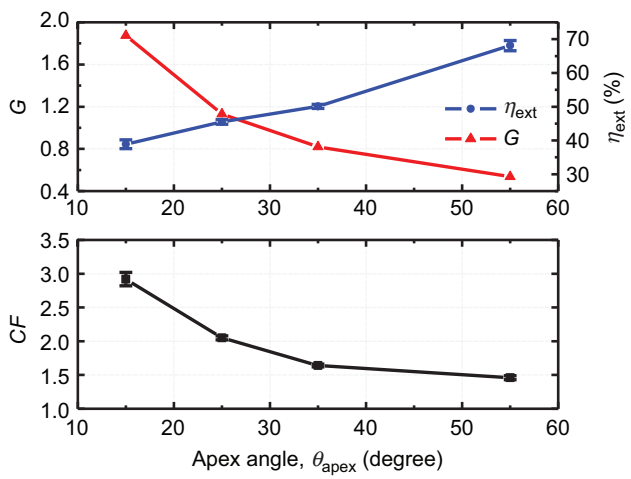

Figure 3 (**a**) Geometric area ratio (*G*), extraction efficiency (η_{ext}) and (**b**) *CF vs.* apex angle (θ_{apex}) at $J=1.0$ mA cm^{-2} for concentrators with θ_{apex} values of 15.5, 25.5, 35.5 and 55.5°. Note that *CF* increases monotonically as θ_{apex} decreases due to the increased number of reflections compared to concentrators with large θ_{apex} values. At the same time, η_{ext} decreases due to increased propagation losses. *CF*, concentration factor.

Table 1 Concentration factor (*CF*)[a] and geometric extraction efficiency (η_{ext}) at a current density (*J*) of 1.0 mA cm^{-2} *vs.* the apex angle (θ_{apex})

θ_{apex} (°)	15.5	25.5	35.5	55.5
CF[b]	2.9±0.1	2.05±0.03	1.64±0.02	1.46±0.03
η_{ext} (%)	38.9±1.3	45.5±0.7	50.1±0.6	68.1±1.5

[a] *CF* is calculated based on the effective luminance from a single panel, assuming that all four panels have identical luminous characteristics.
[b] Errors for *CF* and η_{ext} are standard deviations from at least three single-panel concentrator devices.

Figure 4a shows the normalized luminous intensity of the concentrator with respect to the reference as a function of the viewing angle ϕ measured in the direction parallel to the side (denoted as horizontal) and along the diagonal of the aperture. While the reference is approximately a Lambertian source, the concentrator exhibits a batwing intensity profile where the intensity at viewing angles from $\phi=40$–50° relative to the aperture normal is larger than along the central axis of the concentrator. The resultant luminance distribution[16] is given by

$$I(\phi)=\frac{L(\phi)}{h^2}\cos^3\phi \quad (4)$$

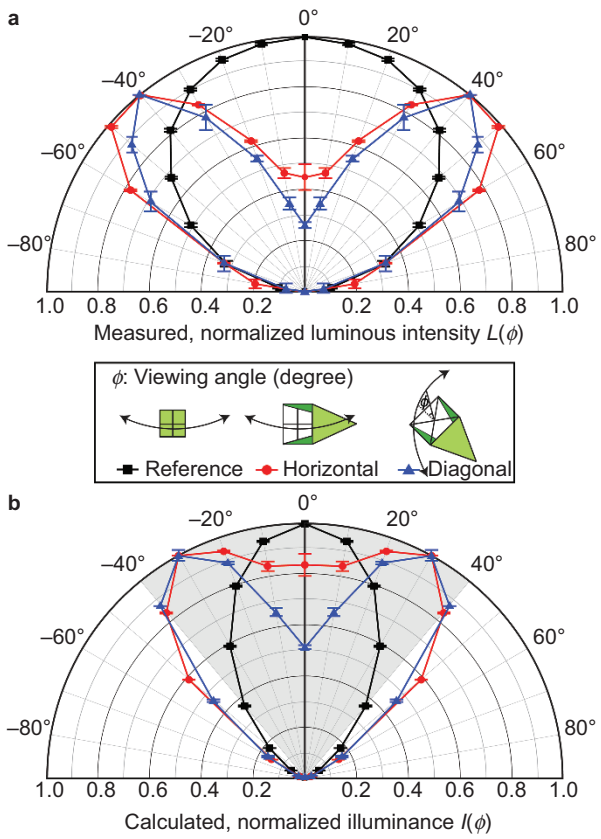

Figure 4 (**a**) Normalized luminous intensity ($L(\phi)$). Also shown is an illustration of the directions along which the intensity profiles of the devices were measured. (**b**) Calculated illuminance $I(\phi)$ of the concentrator with respect to the reference in polar coordinates *vs.* the viewing angle ϕ, as measured in the direction parallel to the side (denoted as horizontal) and along the diagonal of the aperture. The shaded area indicates the zone of nearly uniform illumination achieved by the concentrator along the horizontal axis.

Table 2 Simulated[a] extraction efficiency, average intensity-weighted reflections and exit angles ($\eta_{ext,x}$, $\bar{N}$ and $\bar{\alpha}_{exit}$, respectively) of the exiting rays for two values for PHOLED reflectance (R_{PHOLED}) *vs.* the relative position of the emission (x) from the apex

Position x	R_{PHOLED} (%)	0	0.1	0.2	…	0.8	0.9	1.0
$\eta_{ext,x}$	66	14.2%	15.7%	17.7%	…	43.0%	53.8%	69.3%
	71	18.7%	20.3%	22.5%	…	47.6%	57.4%	71.1%
$\bar{N}$	66	3.63	3.44	3.20	…	1.33	0.84	0.31
	71	3.92	3.71	3.44	…	1.45	0.94	0.37
$\bar{\alpha}_{exit}$	66	1.2°	0.6°	0.5°	…	29.4°	39.1°	51.2°
	71	1.1°	0.6°	0.5°	…	29.7°	39.3°	51.0°

[a] Concentrator height is assumed to be unity and the device reflectance is assumed to be invariant to the incident angle.

at ϕ and distance h. For an arbitrary h, the concentrator produces nearly uniform surface illumination over $\Delta\phi = \pm 40°$, while the reference has a peak illuminance at $\phi = 0°$ that decreases dramatically with ϕ, as shown in Figure 4b. When installed overhead, the profile of the concentrator, unlike the reference, avoids strong veiling reflections from the illuminated surface that result from intense downward emission at low ϕ.

We used a ray-tracing algorithm to model the angular distribution profile of the luminaire and determine N_{ds} from Equation (3). The simulation generates the extraction efficiency ($\eta_{ext,x}$) of the rays emitted at distance x from the vertex of the concentrator, the intensity-weighted average number of reflections $\bar{N}$ required to reach the aperture and the intensity-weighted average exit angles $\bar{\alpha}_{exit}$ relative to the concentrator central axis. Each property for two different PHOLED reflectance values (R_{PHOLED}) is provided in Table 2. The details of the algorithm and the assumptions used are included in Figure S1. Emissions originating from the vertex are strongly attenuated due to the high N_{ds} and therefore do not contribute significantly to the exit luminance. In addition, the $\bar{\alpha}_{exit}$ values of these rays are low, leading to relatively weak intensities along the central axis (cf. Figure 4). However, the rays emitted near the aperture escape with fewer reflections. Thus, their $\bar{\alpha}_{exit}$ values are distributed from 30° to 50°, corresponding to a high intensity peak near 40° in the Luminous intensity profile. A primary factor that determines the $\bar{\alpha}_{exit}$ values and the resultant batwing distribution is the Lambertian emission distribution of the panels, while the reflectance of the device determines the $\eta_{ext,x}$ (Table 2). Hence, we infer that the desired emission profile of the concentrator is achieved by tailoring the profiles of its component PHOLEDs. For example, if the PHOLEDs in the concentrator have relatively intense emission at high angles, we can use microlens arrays[17] or gratings[18] embedded in the substrates to extract emissions with lower $\bar{N}$ values at smaller $\bar{\alpha}_{exit}$. This results in directed or spot illumination profiles.

The geometry of the concentrator also affects the emission profile. A concentrator can produce a higher luminous flux at a low $\bar{\alpha}_{exit}$ with larger aperture (or θ_{apex}) than with a smaller aperture because the rays emitted near the vertex experience fewer reflections with an enlarged escape cone (Supplementary Fig. S2). Additionally, if the side panel angle is large, the emissions near the aperture exit at smaller $\bar{\alpha}_{exit}$ values, while increasing the total η_{ext}. This configuration has a correspondingly decreased geometric area ratio, leading to a reduced *CF* (Figure 3).

An effective means for enhancing both the η_{ext} and *CF* independent of geometry is to increase the PHOLED reflectance (R_{PHOLED}). The PHOLED forms a weak microcavity[19] where the R_{PHOLED} is determined by the reflection, transmission and interference occurring inside the organic thin films and the metal cathodes. Figure 5a and 5b show the R_{PHOLED} as a function of the incident angle θ_{inc} and the wavelength λ calculated for PHOLEDs using Al (denoted as Device A) or Ag (Device B) as the cathode metals, respectively (Supplementary Fig. S3). Because the PHOLED emission is unpolarized,[20] the total reflectance is obtained from the average of the transverse electric and magnetic mode reflectance values at wavelengths ranging from $\lambda = 460$ to 600 nm, corresponding to 90% of the spectral emission

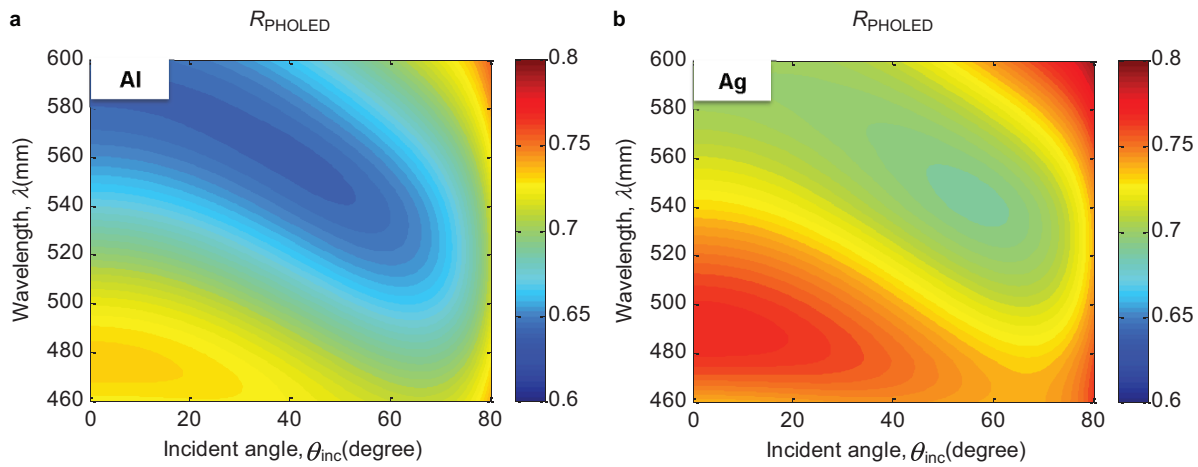

Figure 5 Average of the transverse electric and magnetic mode reflectance values of a PHOLED (R_{PHOLED}, *z*-scale) consisting of a 65-nm-thick hole blocking/electron transport layer (**a**) with an Al cathode and (**b**) with an Ag cathode as a function of the wavelength λ and the angle of incident light θ_{inc}, relative to the surface normal of the PHOLEDs. Here, the reflectance values range from 60% to 80%, as denoted by the blue to red color scale on the right of each contour plot. PHOLED, phosphorescent organic light emitting device.

doi:10.1038/lsa.2014.62

from the green PHOLED at incident angles ranging from θ_{inc}=0–80°. At θ_{inc}>80°, most emissions for both devices are reflected by the polyethylene terephthalate substrate. The reflectance of Device A varies from 64.2%±1.3% to 76.3%±1.2% compared with Device B, which varies from 69.2%±0.6% to 79.9%±2.2% (error is based on the 10% variation of the total thickness of the organic layers). Because Ag has a smaller extinction coefficient than Al, Device B absorbs less and has a higher R_{PHOLED}, as shown in Figure 5. This leads to an increased η_{ext} from the concentrator (Table 2). The high R_{PHOLED} contours in Figure 5 can be spectrally shifted to the PHOLED emission maximum by tuning the thickness of the electron transporting layer and/or the hole transport layer. However, the outcoupling efficiency of the PHOLEDs, which contributes to the total luminous flux of the concentrator, is also dependent on the properties of the microcavities formed between the emission zones and the cathodes (Supplementary Fig. S4). Therefore, R_{PHOLED} can be modified by varying the hole transport layer thickness without significantly changing the outcoupling efficiency. Finally, the incident light that is not reflected is primarily absorbed by the ITO and the cathode. For example, at a normal incidence of λ=522 nm, where the PHOLED emission peaks, the ITO and Al in Device A absorbs 20.0%±1.2% and 10.1%±0.8% of the light, respectively, while the ITO and Ag in Device B absorbs 19.7%±1.7% and 5.1%±0.2%, respectively, considering a 10% variation in the thickness of organic layers.

CONCLUSIONS

We demonstrated concentrated PHOLED emission from a pyramid-shaped luminaire. By increasing the area of the side of the concentrator, a high concentration factor is achieved at the expense of the geometric extraction efficiency due to increased reflections from the surfaces of the devices comprising the edge of the luminaire. To achieve efficient extraction and a high *CF*, increasing the cathode reflectivity is an effective means of increasing the device external luminance efficiency. We observed that the angular intensity profile of the luminaire follows a batwing distribution, making it suitable for uniform downward illumination of surfaces. This concentrator concept can be generally applied to any color of emission (red, green, blue or white), which diversifies the potential lighting applications. To obtain the desired color balance from the concentrator, however, the PHOLED spectral reflectance should be tuned by considering the microcavities and cathode reflectance effects following procedures described here to determine the thickness of the ITO and organic layers. We also noted that while a pyramid shape was used in our demonstration, different concentration factors and emission profiles can be achieved by employing other geometries using this same general design concept. For example, parabolic or compound parabolic concentrator shapes show promise for achieving *CF* values as high as 7. These designs may provide aesthetic advantages over the current design. Hence, our method for concentrating the emission can be advantageously realized in many practical, high intensity OLED-based luminaire configurations.

ACKNOWLEDGEMENTS

The authors acknowledge partial funding support from Universal Display Corporation. The authors thank Sungyong Seo for discussions and assistance with the device simulations.

1 Tang CW, VanSlyke SA. Organic electroluminescent diodes. *Appl Phys Lett* 1987; **51**: 913–915.
2 Baldo MA, Lamansky S, Burrows PE, Thompson ME, Forrest SR. Very high-efficiency green organic light-emitting devices based on electrophosphorescence. *Appl Phys Lett* 1999; **75**: 4–6.
3 National Research Council. *Assessment of Advanced Solid-state Lighting*. Washington, DC: The National Academies Press; 2013.
4 Giebink NC, Forrest SR. Quantum efficiency roll-off at high brightness in fluorescent and phosphorescent organic light emitting diodes. *Phys Rev B* 2008; **77**: 235215–235223.
5 Giebink NC, D'Andrade BW, Weaver MS, Mackenzie PB, Brown JJ *et al*. Intrinsic luminance loss in phosphorescent small-molecule organic light emitting devices due to bimolecular annihilation reactions. *J Appl Phys* 2008; **103**: 044509.
6 Dey TW, Letter EC. Luminaire using a multilayer interference mirror. US4161015 A, 1979.
7 Saccomanno RJ, Steiner IB. Luminaires for artificial lighting. US7195374 B2, 2007.
8 Jacobson BA, Gengelbach RD, Medendorp NW Jr, Roberts L, Perry J. Optical system for batwing distribution. US20090225543 A1, 2009.
9 Kröger M, Hamwi S, Meyer J, Riedl T, Kowalsky W *et al*. Role of the deep-lying electronic states of MoO_3 in the enhancement of hole-injection in organic thin films. *Appl Phys Lett* 2009; **95**: 123301–123303.
10 Qiu J, Wang ZB, Helander MG, Lu ZH. MoO_3 doped 4,4'-N,N'-dicarbazole-biphenyl for low voltage organic light emitting diodes. *Appl Phys Lett* 2011; **99**: 153305–153307.
11 Wang ZB, Helander MG, Qiu J, Puzzo DP, Greiner MT *et al*. Highly simplified phosphorescent organic light emitting diode with >20% external quantum efficiency at >10,000 cd/m^2. *Appl Phys Lett* 2011; **98**: 073310–073312.
12 Wang N, Zimmerman JD, Tong X, Xiao X, Yu J *et al*. Snow cleaning of substrates increases yield of large-area organic photovoltaics. *Appl Phys Lett* 2012; **101**: 133901–133903.
13 Forrest SR, Bradley DD, Thompson ME. Measuring the efficiency of organic light-emitting devices. *Adv Mater* 2003; **15**: 1043–1048.
14 Choi S, Potscavage WJ, Kippelen B. Area-scaling of organic solar cells. *J Appl Phys* 2009; **106**: 054507–054516.
15 Piliego C, Mazzeo M, Salerno M, Cingolani R, Gigli G *et al*. Analysis and control of the active area scaling effect on white organic light emitting diodes towards lighting applications. *Appl Phys Lett* 2006; **89**: 103514–103516.
16 Lindsey JL. *Applied Illumination Engineering*. Lilburn: The Fairmont Press, Inc.; 1997.
17 Möller S, Forrest SR. Improved light out-coupling in organic light emitting diodes employing ordered microlens arrays. *J Appl Phys* 2002; **91**: 3324–3327.
18 Zhang S, Turnbull GA, Samuel ID. Highly directional emission and beam steering from organic light-emitting diodes with a substrate diffractive optical element. *Adv Opt Mater* 2014; **2**: 343–347.
19 Bulović V, Khalfin VB, Gu G, Burrows PE, Garbuzov DZ *et al*. Weak microcavity effects in organic light-emitting devices. *Phys Rev B* 1998; **58**: 3730–3740.
20 Cok R. Organic polarized light emitting diode display with polarizer. US20050088084 A1, 2005.

Supplementary information for this article can be found on the *Light: Science & Applications*' website (http://www.nature.com/lsa/).